

The computed characteristics of turbulent flow and convection in concentric circular annuli. Part III. Alternative thermal boundary conditions

Bo Yu ^a, Yasuo Kawaguchi ^a, Hiroyuki Ozoe ^b, Stuart W. Churchill ^{c,*}

^a National Institute of Advanced Industrial Science and Technology, Tsukuba, Ibaraki 305-8564, Japan

^b Institute of Advanced Material Study, Kyushu University, Kasuga, Fukuoka 816, Japan

^c Department of Chemical and Biomolecular Engineering, University of Pennsylvania, 311A Towne Building, 220 South 33rd Street, Philadelphia, PA 19104, USA

Received 26 December 2003; received in revised form 4 August 2004

Available online 11 November 2004

Abstract

Numerically predicted values of the Nusselt number are presented for annuli with uniform heating of the outer surface only, uniform equal heating of both surfaces, and uniform heating of one surface and equal cooling of the other. Results are also presented for a parallel-plate channel with isothermal heating of one wall and equal isothermal heating of both walls. The predictions are based on semi-theoretical expressions for the dimensionless turbulent shear stress but are insensitive to the limited empiricism within the model for convection. The predicted values of Nu are in good agreement with the somewhat limited experimental data for these less frequently encountered thermal boundary conditions. The results encompass all values of the Prandtl number and all values of the Reynolds number of practical concern. These values, together with those in a preceding paper for uniform heating of the inner wall only, and together with the generalizations described in a succeeding paper, permit the accurate prediction of the Nusselt number from theoretically based algebraic expressions for essentially all of the thermal conditions that result in fully developed convection.

© 2004 Elsevier Ltd. All rights reserved.

1. Introduction

The most important application of turbulent convection in an annulus is as the outer channel of a double-pipe heat exchanger with countercurrent flow. This behavior is closely represented by the idealized condition of fully developed convection in the fully developed flow of a

fluid with invariant physical properties, a uniform heat flux across the inner tube wall, and perfect insulation on the outer wall. As a first step in modeling this behavior, an essentially exact solution was developed by Kaneda et al. [1] for fully developed turbulent flow in a concentric circular annulus for all aspect ratios by means of the step-wise numerical integration of a differential model in which the turbulent shear stress was represented directly by algebraic expressions constructed from theoretically structured asymptotes. As contrasted with the prior use of this methodology for a round tube and a parallel-plate channel, empirical expressions were necessarily

* Corresponding author. Tel.: +1 215 898 5579; fax: +1 215 573 2093.

E-mail address: churchil@seas.upenn.edu (S.W. Churchill).

Nomenclature

a	radius of annulus (m)
a^+	dimensionless radius of annulus [$a(\tau_w \rho)^{1/2} / \mu$]
c	specific heat capacity (J/kg K)
h	heat transfer coefficient [$j_w / (T_w - T_m)$] (W/m ² K)
k	thermal conductivity (W/m K)
j	radial heat flux density (W/m ²)
Nu	Nusselt number [$2h(a_2 - a_1) / k$]
Nu_0	$Nu \{ Pr = 0 \}$
Nu_1	$Nu \{ Pr = Pr_t \}$
Nu^*	$2j_w(a_2 - a_1) / k(T_1 - T_2)$
Pr	Prandtl number [$c\mu/k$]
Pr_t	turbulent Prandtl number
	$\left[\frac{Pr(\overline{u'v'})^{++} (1 - (\overline{T'v'})^{++})}{(\overline{T'v'})^{++} (1 - (\overline{u'v'})^{++})} \right]$
R	radius ratio [r/a_1]
Re	Reynolds number [$2(a_1 - a_2)u_m / \mu$]
T	temperature (K)
T^+	$k(\rho\tau_{w1})^{1/2}(T_{w1} - T) / \mu j_{w1}$
u	axial component of time-averaged velocity (m/s)
u^+	dimensionless axial velocity [$u / (\rho\tau_{w1})^{1/2}$]
u_m	mixed-mean axial velocity (m/s)
$\overline{u'v'}$	time-averaged product of fluctuating components of the velocity

$(\overline{u'v'})^+$	dimensionless shear stress [$-\rho(\overline{u'v'}) / \tau_w$]
$(\overline{u'v'})^{++}$	fraction of local total shear stress due to turbulence [$-\rho(\overline{u'v'}) / \tau$]
$\overline{T'v'}$	time-averaged product of fluctuating temperature and radial velocity
$(\overline{T'v'})^{++}$	fraction of total local radial heat flux density due to turbulence $\rho c (\overline{T'v'}) / j$
μ	dynamic viscosity (Pa s)
ρ	specific density (kg/m ³)
τ	shear stress (Pa)

Subscripts

A	adiabatic
H	uniformly heated on one wall
HC	uniformly and equally heated and cooled ($j_{w1}a_1 = -j_{w2}a_2$)
HH	uniformly and equally heated on both walls ($j_{w1}a_1 = j_{w2}a_2$)
i	on inner surface
m	mean value
o	on outer surface
T	isothermally heated
w1	based on the inner wall
w2	based the outer wall
wm	based on mean shear stress on the walls

introduced for the location of the zero in the total shear stress and for the maximum in the velocity distribution within the annulus. The excellent agreement of the predictions of the time-averaged velocity distribution and the mixed-mean velocity (and thereby the overall friction factor) with experimental data implies that the error introduced by these two empirical expressions and by the empirical coefficients in the representation for the turbulent shear stress is negligible for all practical purposes. Algebraic predictive equations based on the same asymptotes reproduce the computed values of the time-averaged velocity distribution and the mixed-mean velocity almost exactly. These expressions are properly designated as “predictive” rather than “correlative” because they were formulated without reference to the computed or experimental values themselves. Step-wise numerical solutions were next carried out by Yu et al. [2] for fully developed convection in fully developed flow with uniform heating of the inner surface only, which is the most important case from a practical point of view. These numerical solutions were based on integration of the differential energy balance using an empirical expression for the local fraction of the radial transport of energy due to turbulence. The computations encompassed a complete range of values of Pr , a wide range of values of Re , and

a wide range of aspect ratios. The computed values of Nu were found to be fortuitously insensitive to the uncertainty introduced by the single added empiricism beyond that for flow, namely an expression for the turbulent Prandtl number, and to be in good agreement with experimental data for air, water, and mercury. Generalized algebraic predictive equations were devised to represent the computed values of Nu in terms of Nu_0 , Nu_1 , and Nu_∞^1 .

Numerically computed solutions for Nu are presented herein for several other thermal boundary conditions for annuli, namely, (1) uniform heating on the outer surface only, (2) equal uniform heat fluxes on the two surfaces, and (3) uniform heating on one surface with equal cooling on the other. It should be noted that the behavior for equal uniform heating and cooling is equivalent to that for unequal uniform temperatures in that, as contrasted with all the other cases, the fluid temperature does not then vary longitudinally. Values of Nu are also presented for parallel-plate channels (annuli with an aspect ratio of unity) for two additional conditions, namely, isothermal heating on one surface only and equal isothermal heating on both surfaces.

A uniform wall temperature may be closely attained by boiling or condensation on the inner or outer surfaces of

an annulus owing to the higher heat transfer coefficients for these two processes as compared to the coefficients for the transfer of sensible heat by forced convection. Uniform heating of a surface may be attained electrically or

be approached for isoenthalpic countercurrent flow in double- or triple-pass annular exchangers. Thus all of the thermal boundary conditions considered have some practical interest, at least in an asymptotic sense.

Table 1
Computed values of Nu_0 for uniform heating of the outer surface only

a_1/a_2	0.01	0.05	0.1	0.2	0.5	0.8	0.9	0.95	0.99	0.999
$(a_2^+ - a_1^+)_{w1}$	Nu_{0oHA}									
500	5.303	5.332	5.36	5.415	5.574	5.689	5.717	5.730	5.739	5.741
800	5.353	5.384	5.405	5.456	5.609	5.721	5.748	5.760	5.769	5.771
1000	5.381	5.403	5.423	5.471	5.623	5.733	5.76	5.772	5.781	5.783
2000	5.442	5.451	5.466	5.51	5.656	5.762	5.788	5.8	5.808	5.810
5000		5.494	5.506	5.546	5.685	5.788	5.813	5.824	5.832	5.833
10,000		5.521	5.529	5.566	5.702	5.802	5.826	5.836	5.844	5.846
20,000			5.548	5.583	5.715	5.812	5.836	5.846	5.854	5.855
50,000			5.569	5.601	5.728	5.823	5.846	5.856	5.863	5.864
100,000			5.582	5.611	5.735	5.828	5.85	5.859	5.866	5.868
200,000				5.619	5.739	5.829	5.85	5.859	5.866	5.867
500,000				5.621	5.734	5.819	5.839	5.847	5.853	5.855

Table 2
Computed values of Nu_1 for uniform heating of the outer surface only

a_1/a_2	0.01	0.05	0.1	0.2	0.5	0.8	0.9	0.95	0.99	0.999
$(a_2^+ - a_1^+)_{w1}$	Nu_{1oHA}									
500	33.69	37.66	39.22	40.60	41.98	42.30	42.30	42.29	42.27	42.27
800	50.49	57.17	59.80	61.93	64.03	64.55	64.57	64.56	64.55	64.54
1000	61.14	69.98	73.20	75.77	78.33	79.00	79.04	79.03	79.02	79.01
2000	114.0	132.3	137.8	142.2	147.0	148.5	148.6	148.7	148.7	148.7
5000		311.1	320.2	328.8	339.8	344.0	344.6	344.8	345.0	344.9
10,000		583.4	608.8	622.5	643	651.8	653.5	654.1	654.5	654.4
20,000			1162	1182	1220	1239	1243	1244	1245	1245
50,000			2750	2776	2860	2907	2917	2921	2924	2925
100,000			5206	5317	5465	5558	5579	5588	5595	5596
200,000				10,240	10,480	10,660	10,700	10,720	10,730	10,730
500,000				24,660	24,980	25,340	25,430	25,470	25,490	25,490

Table 3
Computed values of Nu_{0i} for equal uniform heating on both surfaces

a_1/a_2	0.01	0.05	0.1	0.2	0.5	0.8	0.9	0.95	0.99	0.999
$(a_2^+ - a_1^+)_{w1}$	Nu_{0iHH}									
500	61.65	21.87	15.33	11.67	9.678	9.775	9.948	10.05	10.14	10.17
800	61.78	21.91	15.37	11.72	9.77	9.922	10.12	10.23	10.33	10.36
1000	61.77	21.92	15.39	11.74	9.805	9.978	10.18	10.3	10.41	10.43
2000	61.8	21.95	15.42	11.78	9.885	10.11	10.34	10.47	10.59	10.61
5000		21.97	15.44	11.81	9.951	10.23	10.47	10.62	10.74	10.77
10,000		21.97	15.45	11.82	9.987	10.29	10.55	10.7	10.83	10.86
20,000			15.45	11.83	10.01	10.35	10.61	10.77	10.91	10.94
50,000			15.46	11.84	10.05	10.41	10.69	10.85	11.00	11.03
100,000			15.46	11.85	10.07	10.46	10.75	10.92	11.06	11.10
200,000				11.86	10.11	10.51	10.82	10.99	11.14	11.18
500,000				11.89	10.17	10.62	10.94	11.13	11.29	11.33

In the interests of convenience and clarity, the limited experimental data and prior numerical solutions for uniform heating of the outer wall and for uniform heating

but unequal heating on both walls are discussed in the context of comparisons with the new computed results rather than here in advance.

Table 4
Computed values of Nu_{1i} for equal uniform heating for both surfaces

a_1/a_2	0.01	0.05	0.1	0.2	0.5	0.8	0.9	0.95	0.99	0.999
$(a_2^+ - a_1^+)_{w1}$	Nu_{1iHH}									
500	102.8	51.42	48.48	47.50	49.54	52.49	53.50	54.00	54.41	54.50
800	106.0	79.01	74.72	72.77	75.28	79.42	80.84	81.55	82.12	82.25
1000	121.8	97.51	91.88	89.17	91.93	96.83	98.52	99.37	100.0	100.2
2000	231.1	189.6	175.1	168.0	171.8	180.2	183.0	184.5	185.7	185.9
5000		465.1	412.8	389.7	395.2	412.7	418.7	421.7	424.1	424.7
10,000		871.9	792.6	739.5	745.6	776.3	787.0	792.3	796.4	797.4
20,000			1529	1408	1412	1466	1485	1494	1501	1503
50,000			3683	3322	3300	3416	3455	3475	3491	3494
100,000			6975	6397	6306	6506	6576	6611	6638	6644
200,000				12,420	12,110	12,450	12,570	12,640	12,680	12,690
500,000				30,640	29,110	29,700	29,940	30,060	30,160	30,180

Table 5
Computed values of Nu_{0o} for equal uniform heating on both surfaces

a_1/a_2	0.01	0.05	0.1	0.2	0.5	0.8	0.9	0.95	0.99	0.999
$(a_2^+ - a_1^+)_{w1}$	Nu_{0oHH}									
500	16.32	16.57	16.21	15.19	12.54	10.91	10.51	10.33	10.20	10.17
800	17.55	17.5	17.05	15.87	12.92	11.15	10.73	10.54	10.40	10.36
1000	17.92	17.88	17.39	16.14	13.08	11.25	10.81	10.62	10.47	10.44
2000	18.96	18.84	18.24	16.82	13.45	11.48	11.02	10.81	10.65	10.62
5000		19.70	19.01	17.44	13.79	11.69	11.20	10.98	10.81	10.78
10,000		20.16	19.45	17.80	13.98	11.80	11.30	11.07	10.90	10.86
20,000			19.8	18.09	14.13	11.90	11.38	11.14	10.97	10.93
50,000			20.19	18.42	14.30	12.00	11.46	11.22	11.04	11.00
100,000				20.45	18.63	14.41	12.05	11.51	11.08	11.04
200,000					18.82	14.50	12.09	11.54	11.29	11.07
500,000					19.04	14.56	12.10	11.53	11.28	11.06

Table 6
Computed values of Nu_{1o} for equal uniform heating for both surfaces

a_1/a_2	0.01	0.05	0.1	0.2	0.5	0.8	0.9	0.95	0.99	0.999
$(a_2^+ - a_1^+)_{w1}$	Nu_{1oHH}									
500	48.39	73.14	73.54	69.90	61.58	56.76	55.56	55.02	54.60	54.51
800	80.63	105.0	105.4	102.2	91.92	85.38	83.73	82.98	82.40	82.27
1000	105.5	123.6	125.4	122.8	111.5	103.9	101.9	101.0	100.4	100.2
2000	180.5	205.1	218.4	220.6	204.4	192.0	188.8	187.3	186.2	185.9
5000		407.0	466.7	487.5	461.4	436.7	430.3	427.3	425.1	424.6
10,000		761.7	839.2	896.5	859.4	817.6	806.6	801.6	797.7	796.9
20,000			1518	1657	1608	1536	1518	1509	1502	1501
50,000			3332	3751	3699	3554	3516	3498	3485	3482
100,000			6341	6967	6966	6724	6658	6627	6604	6599
200,000				12,910	13,130	12,740	12,630	12,580	12,540	12,530
500,000				28,760	30,300	29,670	29,470	29,370	29,300	29,280

2. Methodology

The differential model for all of the processes considered herein is identical to that utilized by Yu et al. [2] for uniform heating of the inner wall of an annulus and,

therefore, is not reproduced here. However, except for heating on one wall only and for a parallel-plate channel heated uniformly and equally on both walls, an iterative procedure was required for the numerical integration owing to the second thermal boundary condition, and,

Table 7
Computed values of Nu_{0i} for equal isothermal heating and cooling

a_1/a_2	0.01	0.05	0.1	0.2	0.5	0.8	0.9	0.95	0.99	0.999
$(a_2^+ - a_1^+)_{w1}$	Nu_{0iHC}									
500	45.37	14.18	9.253	6.480	4.652	4.171	4.078	4.037	4.007	4.001
800	45.37	14.16	9.243	6.475	4.652	4.172	4.078	4.037	4.007	4.001
1000	45.33	14.15	9.239	6.473	4.652	4.172	4.078	4.037	4.007	4.001
2000	45.25	14.14	9.228	6.467	4.651	4.172	4.078	4.038	4.007	4.001
5000		14.12	9.214	6.459	4.649	4.172	4.078	4.038	4.008	4.001
10,000		14.10	9.205	6.454	4.648	4.172	4.079	4.038	4.008	4.001
20,000			9.197	6.450	4.647	4.172	4.079	4.038	4.008	4.002
50,000			9.188	6.445	4.646	4.173	4.080	4.039	4.009	4.003
100,000			9.183	6.443	4.647	4.175	4.082	4.041	4.011	4.005
200,000				6.443	4.650	4.178	4.085	4.045	4.015	4.008
500,000				6.449	4.660	4.189	4.096	4.055	4.025	4.019

Table 8
Computed values of Nu_{1i} for equal isothermal heating and cooling

a_1/a_2	0.01	0.05	0.1	0.2	0.5	0.8	0.9	0.95	0.99	0.999
$(a_2^+ - a_1^+)_{w1}$	Nu_{1iHC}									
500	94.26	42.52	38.40	35.86	34.57	34.54	34.54	34.53	34.52	34.52
800	96.85	66.54	60.40	55.99	53.48	53.23	53.18	53.14	53.12	53.11
1000	110.7	82.94	74.96	69.14	65.78	65.40	65.32	65.28	65.24	65.23
2000	214.7	166.6	146.5	132.8	125.2	124.3	124.1	124.0	123.9	123.9
5000		428.2	355.0	314.5	293.9	291.6	291.1	290.9	290.7	290.6
10,000		805.3	694.8	604.5	561.7	557.2	556.6	556.2	555.9	555.6
20,000			1367	1165	1076	1068	1067	1066	1066	1065
50,000			3391	2794	2554	2534	2531	2530	2529	2529
100,000			6414	5461	4938	4892	4888	4886	4884	4883
200,000				10,810	9618	9503	9491	9486	9479	9478
500,000				27,830	23,740	23,250	23,190	23,150	23,120	23,110

Table 9
Computed values of Nu_{0o} for equal isothermal heating and cooling

a_1/a_2	0.01	0.05	0.1	0.2	0.5	0.8	0.9	0.95	0.99	0.999
$(a_2^+ - a_1^+)_{w1}$	Nu_{0oHC}									
500	3.166	3.177	3.211	3.295	3.584	3.848	3.926	3.964	3.993	3.999
800	3.158	3.181	3.212	3.294	3.582	3.847	3.926	3.963	3.993	3.999
1000	3.166	3.183	3.212	3.294	3.582	3.847	3.926	3.963	3.993	3.999
2000	3.176	3.186	3.215	3.295	3.581	3.846	3.925	3.963	3.993	3.999
5000		3.192	3.219	3.297	3.581	3.846	3.925	3.963	3.993	3.999
10,000		3.198	3.223	3.299	3.581	3.846	3.925	3.963	3.992	3.999
20,000			3.226	3.301	3.581	3.846	3.925	3.963	3.992	3.998
50,000			3.23	3.303	3.581	3.845	3.924	3.961	3.991	3.997
100,000			3.232	3.303	3.58	3.843	3.922	3.96	3.989	3.995
200,000				3.302	3.578	3.84	3.919	3.956	3.985	3.992
500,000				3.297	3.57	3.831	3.909	3.946	3.975	3.982

Table 10
Computed values of Nu_{1o} for equal isothermal heating and cooling

a_1/a_2	0.01	0.05	0.1	0.2	0.5	0.8	0.9	0.95	0.99	0.999
$(a_2^+ - a_1^+)_{w1}$	Nu_{1oHC}									
500	25.84	25.36	26.74	28.61	31.85	33.71	34.15	34.34	34.48	34.51
800	36.75	39.28	41.74	44.44	49.13	51.89	52.55	52.84	53.05	53.10
1000	43.05	48.80	51.68	54.78	60.37	63.74	64.54	64.90	65.16	65.21
2000	83.26	97.60	100.6	104.9	114.7	121.0	122.5	123.2	123.7	123.8
5000		251.8	243.7	248.1	268.9	283.7	287.4	289.0	290.3	290.5
10,000		472.8	477.7	476.8	513.7	542	549.2	552.4	554.9	555.2
20,000			941.1	919.1	983.6	1038	1052	1058	1063	1064
50,000			2341	2203	2331	2459	2493	2508	2519	2522
100,000			4415	4299	4496	4737	4801	4831	4853	4857
200,000				8479	8719	9158	9280	9335	9375	9384
500,000				21,590	21,240	22,110	22,370	22,480	22,560	22,570

in the case of one or more isothermal walls, to the presence of the mixed-mean temperature in the expression for the local heat flux density.

The local heat flux density ratio in the fluid, which occurs in the differential energy balance, is different for the several modes of heating. It may be expressed in general as

$$\frac{j}{j_{w1}} = -\frac{j_{w2}}{j_{w1}} + \frac{\left(1 + \frac{j_{w2}}{j_{w1}}\right)}{R \left[\left(a_2/a_1\right)^2 - 1 \right]} \int_{R^2} \left(\frac{u}{u_m}\right) dR^2, \quad (1)$$

where $R = r/a_1$.

For uniform heating of the inner wall only ($j_{w2} = 0$), as considered by Yu et al. [2], Eq. (1) reduces to

$$\frac{j}{j_{w1}} = \frac{1}{R \left[\left(a_2/a_1\right)^2 - 1 \right]} \int_{R^2} \left(\frac{u}{u_m}\right) dR^2. \quad (2)$$

For equal uniform overall heating of both walls ($j_{w1a1} = j_{w2a2}$) it becomes

$$\frac{j}{j_{w1}} = -\frac{a_1}{a_2} + \frac{1}{R \left[\left(a_2/a_1\right) - 1 \right]} \int_{R^2} \left(\frac{u}{u_m}\right) dR^2 \quad (3)$$

while for uniform equal heating and cooling ($j_{w1a1} = -j_{w2a2}$), it reduces to

$$\frac{j}{j_{w1}} = \frac{1}{R}. \quad (4)$$

3. Numerical integrations

Numerical integrations for uniform heating on the outer wall and for combined uniform heating and cooling were carried out for a series of values of the aspect ratio extending from 0.01 to 0.999, but the calculations for isothermal heating were limited to parallel plates. In all instances the integrations were carried out for 25

values of Pr , extending from 0 to 10,000, and a wide range of values of $(a_2^+ - a_1^+)_{w1}$, extending from the presumed minimum of 150 for fully developed turbulent flow up to 500,000, which corresponds to $Re \cong 30,000,000$ and is obviously greater than any value of practical interest.

Although the complete distribution of the temperature was determined by step-wise numerical integration, and then the mixed-mean temperature by integration of those values, weighted by the velocity, over the cross-section, the thermal results are presented only in terms of Nu and T_{w2}^+ , the dimensionless temperature of the outer surface. Because the generalized, algebraic predictive expressions of Churchill and Zajic [3], as described in slightly improved form by Yu et al. [2], require numerical values only for $Nu_0 = Nu\{Pr = 0\}$ and $Nu_1 = Nu\{Pr = Pr_t\} \cong 0.8673$, and the tabulations herein are limited to these two quantities. However, computed values of the Nu for all 25 of the values of Pr are presented graphically.

Table 11
Computed values of Nu for parallel-plate channels and isothermal heating

b^+	Nu_{0TA}	Nu_{1TA}	Nu_{0TT}	Nu_{1TT}
150	4.918	25.75	8.652	34.46
500	4.926	76.53	8.953	99.14
800	4.927	117.7	9.023	150.9
1000	4.928	144.5	9.050	184.5
2000	4.929	274.0	9.119	344.9
5000	4.930	640.6	9.188	793.4
10,000	4.931	1221	9.230	1496
20,000	4.931	2333	9.266	2830
50,000	4.932	5505	9.307	6598
100,000	4.932	10,560	9.335	12,550
200,000	4.932	20,290	9.360	23,940
500,000	4.933	48,220	9.389	56,380

For computational convenience the numerical integrations were carried out for a series of values of $(a_2^+ - a_1^+)_{w1}$ rather than Re as well for a series of values of a_1/a_2 . Yu et al. [2] provide a tabulation of the corresponding values of Re , $(u_m^+)_{wm}$, and τ_{w1}/τ_{wm} for each listed value of a_1/a_2 , and $(a_2^+ - a_1^+)_{w1}$, and Kaneda et al. [1] present algebraic expressions from which these quantities may be calculated for intermediate values of $(a_2^+ - a_1^+)_{w1}$ and intermediate or lower values of a_1/a_2 . The numerical integrations extended from $(a_2^+ - a_1^+)_{w1}$ of 150 up to 500,000, but the values of Re and $(u_m^+)_{wm}$ in the aforementioned tabulation are omitted for the bordering conditions in which, (1) the value of a matching coefficient in the differential model was suspect, (2) the attainment of fully turbulent flow was uncertain, or (3) the convergence of the numerical values of the time-mean velocity was uncertain. The values of Nu computed numerically in the current work were omitted from the tabulations herein for the same conditions, just as they were by Yu et al. [2], on the premise that any error in the time-mean velocity distribution will influence the time-mean temperature distribution and thereby Nu .

4. Numerical results

Numerically computed values of Nu_{0oHA} and Nu_{1oHA} for uniform heating on the outer surface only are listed in Tables 1 and 2, respectively; of Nu_{0iHH} and Nu_{1iHH} in

Tables 3 and 4, and of Nu_{0oHH} and Nu_{1oHH} in Tables 5 and 6 for equal uniform heating on both surfaces; of Nu_{0iHC} and Nu_{1iHC} in Tables 7 and 8, and of Nu_{0oHC} and Nu_{1oHC} in Tables 9 and 10 for equal uniform heating and cooling. Values of Nu_{0TA} and Nu_{1TA} for isothermal heating of one parallel plate and of Nu_{0TT} and Nu_{1TT} for equal isothermal heating of both plates are listed in Table 11. Here, the subscripts 0 and 1 on Nu designate, as already mentioned, $Pr = 0$ and $Pr = Pr_i$, respectively, o and i designate the inner and outer surfaces, respectively, and H, C, T, and A designate uniformly heated, uniformly cooled, isothermally heated, and adiabatic surfaces, respectively, while HH designates equal heating, HC equal heating and cooling, and TT equal temperatures on the two surfaces.

It should be noted that the tabulated values of Nu are based on heat transfer between the temperature of the indicated wall and the mixed-mean temperature of the fluid stream. For heat transfer directly across the fluid with no longitudinal change in the temperature of the fluid, as in Tables 9 and 10, an alternative, and in some sense a more meaningful quantity, for the case of $Pr = 0$ is Nu^* based on the temperature difference between the two walls. This limiting quantity is given for laminar flow by the following exact solution:

$$Nu^* = \frac{2\left(\frac{a_2}{a_1} - 1\right)}{\ln\left\{\frac{a_2}{a_1}\right\}} \tag{5}$$

Table 12

Fractional approach of surface temperature to mixed-mean value for uniform isothermal heating on the other wall of a parallel-plate channel

a_1/a_2	0.01	0.05	0.1	0.2	0.5	0.8	0.999
$(a_2^+ - a_1^+)_{w1}$	$Pr = Pr_i \cong 0.8673, j_2 = 0$						
800		0.0288	0.0483	0.0805	0.1481	0.2000	0.2153
1000	0.0080	0.0279	0.0470	0.0788	0.1454	0.1892	0.2114
2000	0.0068	0.0238	0.0428	0.0741	0.1385	0.1798	0.2003
5000		0.0169	0.0374	0.0689	0.1307	0.1688	0.1875
10,000		0.0168	0.0334	0.0653	0.1264	0.1614	0.1787
20,000			0.0291	0.0617	0.1205	0.1545	0.1707
	$Pr = Pr_i \cong 0.8673, j_2 a_2 / j_1 a_1 = 0.10$						
800		0.0348	0.0589	0.0996	0.1937	0.2664	0.3086
1000	0.0098	0.0339	0.0577	0.0981	0.1914	0.2633	0.3048
2000	0.0091	0.0303	0.0539	0.0939	0.1849	0.2544	0.2944
5000		0.0240	0.0489	0.0891	0.1777	0.2440	0.2821
10,000		0.0239	0.0452	0.0858	0.1729	0.2371	0.2737
20,000			0.0413	0.0826	0.1683	0.2307	0.2662
	$Pr = 0, j_2 a_2 / j_1 a_1 = 0.10$						
800		0.1239	0.1632	0.2247	0.3613	0.4634	0.5195
1000	0.0765	0.1243	0.1638	0.2256	0.3628	0.4657	0.5221
2000	0.0769	0.1251	0.1649	0.2273	0.3668	0.4710	0.5284
5000		0.1257	0.1657	0.2287	0.3698	0.4756	0.5339
10,000		0.1258	0.1660	0.2293	0.3715	0.4779	0.5393
20,000			0.1661	0.2299	0.3728	0.4806	0.5393

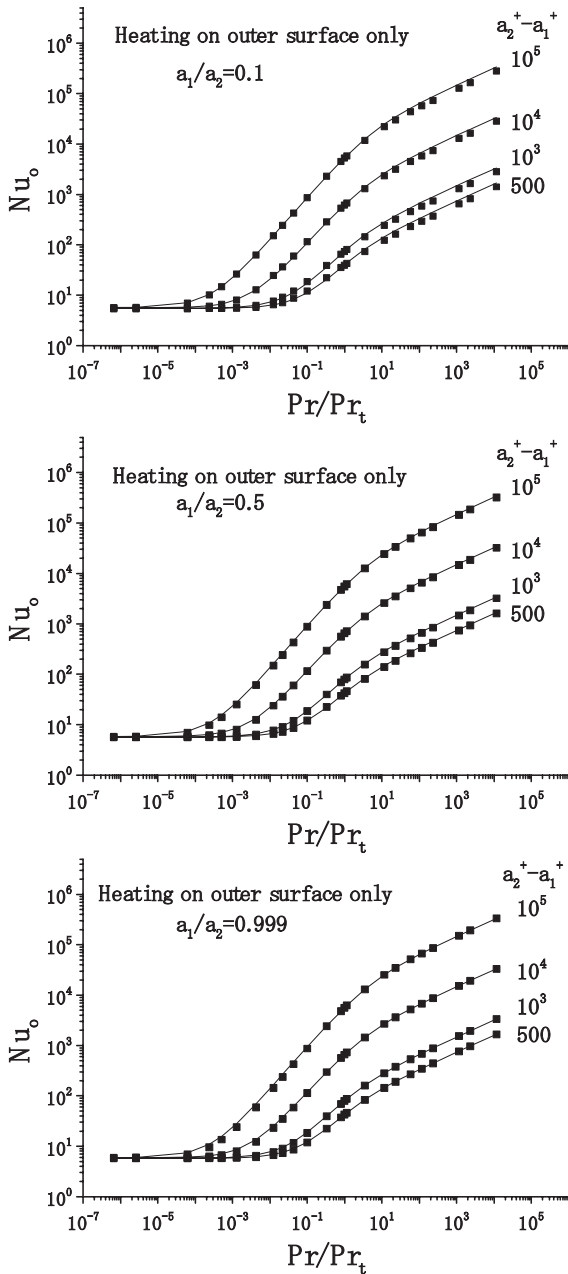


Fig. 1. Representation of the numerically computed values of Nu for uniform heating of the outer wall of an annulus by the predictive equations of Churchill and Zajic [3].

In the limit of $a_2/a_1 \rightarrow 1$, $Nu^* \rightarrow 2$, which differs from the limiting value of ~ 4 in Tables 7 and 10 because of the doubled temperature difference. The value of Nu_0 approaches 4 as $a_2/a_1 \rightarrow 1$ because $T_m \rightarrow (T_1 + T_2)/2$ regardless of the velocity distribution.

The values of Nu in Tables 1–12, together with those of Yu et al. [2] for uniform inner heating only, namely,

Nu_{iHA} , encompass, by virtue of superposition, as discussed by Yu et al. [4], the final paper in this series, all aspects of fully developed convection in annuli except for isothermal heating on one or both walls for a_1/a_2 less than unity.

5. Graphical representations

The computed values of Nu for 25 values of Pr/Pr_t are compared in Figs. 1–4 with the generalized, predictive equations of Churchill and Zajic [3] for all geometries and thermal boundary conditions, as slightly rearranged by Yu et al. [2]. The agreement is very good for all of the conditions, and justifies the tabulation herein of values of Nu_0 and Nu_1 only.

5.1. Comparisons of computed values of Nu with experimental data and prior computed values

Experimental data for heating on the outer surface or on both surfaces are scarcer than those for heating only on the inner surface, the condition examined by Yu et al. [2]. Those of Leung [5], Vilemas et al. [6], and Petukhov and Roizen [7] for air, and of Monrad and Pelton [8] for water are plotted in Fig. 5 versus the values predicted herein. These “predicted” values were obtained by interpolation of the computed values of Nu . The values of Monrad and Pelton fall consistently below the predictions based on the numerical integrations. The values of the other investigators suggest a slightly greater rate of increase with the magnitude of Nu and hence with Re . However, the overall agreement is good. The prior numerically computed values of Kays and Leung [9] for uniform outer heating and $Pr = 0.7$ may also be seen to be in good agreement with the new predictions.

On the other hand, as indicated in Fig. 6, the single set of experimental values for unequal uniform heating ($j_{w1}a_1 = 1.29j_{w2}a_2$) of air by Vilemas et al., for Nu_i fall significantly below the predictions, while those for Nu_o fall slightly above.

5.2. Implementation

The predictions of Nu as a function of Pr/Pr_t are independent of the dependence of Pr_t on Pr , but an expression for this dependence is obviously required to determine numerical values of Nu . As discussed by Churchill [10], the existing expressions for Pr_t are quite uncertain, but, as demonstrated by Yu et al. [11] for round tubes, the predicted values of Nu are fortuitously insensitive to Pr_t , and thereby to this uncertainty.

Eqs. (21) and (22) of Yu et al. [11] predict Nu as a function of Nu_0 , Nu_1 , Nu_∞^1 , and Pr/Pr_t with virtually no empiricism. Nu_∞^1 is subject to a small degree of uncer-

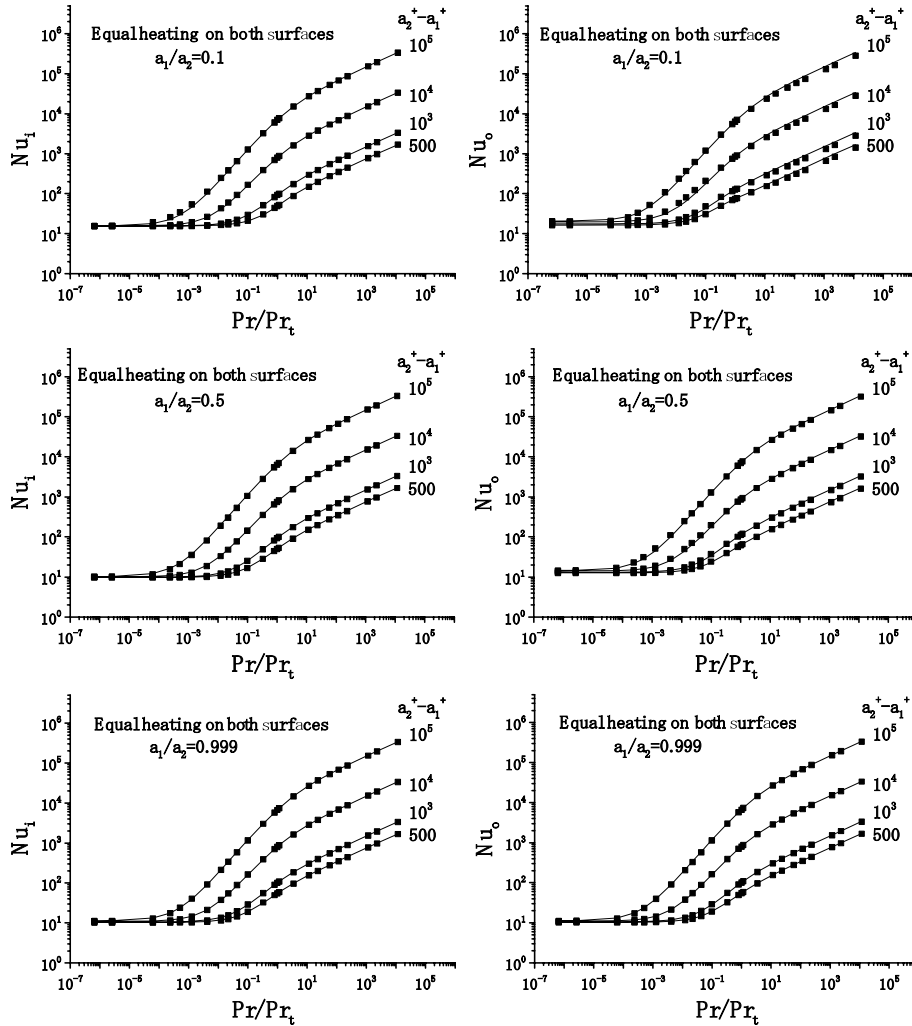


Fig. 2. Representation of the numerically computed values of Nu for uniform equal heating of the walls of an annulus by the predictive equations of Churchill and Zajic [3].

tainty in the coefficient 0.07343, which was determined from direct numerical simulations of the flow, and to the minor uncertainties in $(u_m^+)_{wm}$, as determined by the numerical integrations or from the predictive equation of Kaneda et al. [1]. Finally, some empiricism and uncertainty is associated with the prediction of τ_{wm}/τ_{w1} and thereby in the determination of Re and $(u_m^+)_{wm}$ for a chosen value $(a_2^+ - a_1^+)_{w1}$.

5.3. Surface temperature of outer wall

The temperature of the outer wall is of practical interest in two different contexts, first as a controlling factor in the heat losses to the surroundings, and second in terms of the safety of personnel from burns on contact. The effect of thermal insulation will not be consid-

ered here since turbulent convection in annuli does not introduce anything novel in this respect.

The numerical integrations for the temperature distribution yielded the dimensionless temperature T_{w2}^+ on bare outer surface, and this value, together with the corresponding mixed-mean value T_m^+ , were utilized to calculate the quantity $\frac{T_{w2}^+}{T_m^+} - 1 = \frac{T_m - T_{w2}}{T_{w1} - T_m}$. Values are listed in Table 12 for three representative conditions, namely $Pr = Pr_t \cong 0.8673$ with heat losses of 0% and 10%, and $Pr = 0$ with heat losses of 10%. The quantity $\frac{T_m - T_{w2}}{T_{w1} - T_m}$ represents the difference between the mixed-mean and outer-wall temperature as a fraction of the difference between the inner-wall and mixed-mean temperature. The values for $j_2 = 0$, indicate the decrease in the outer-wall temperature due to imperfect transport of energy in the fluid and those for a heat loss of 10% to the

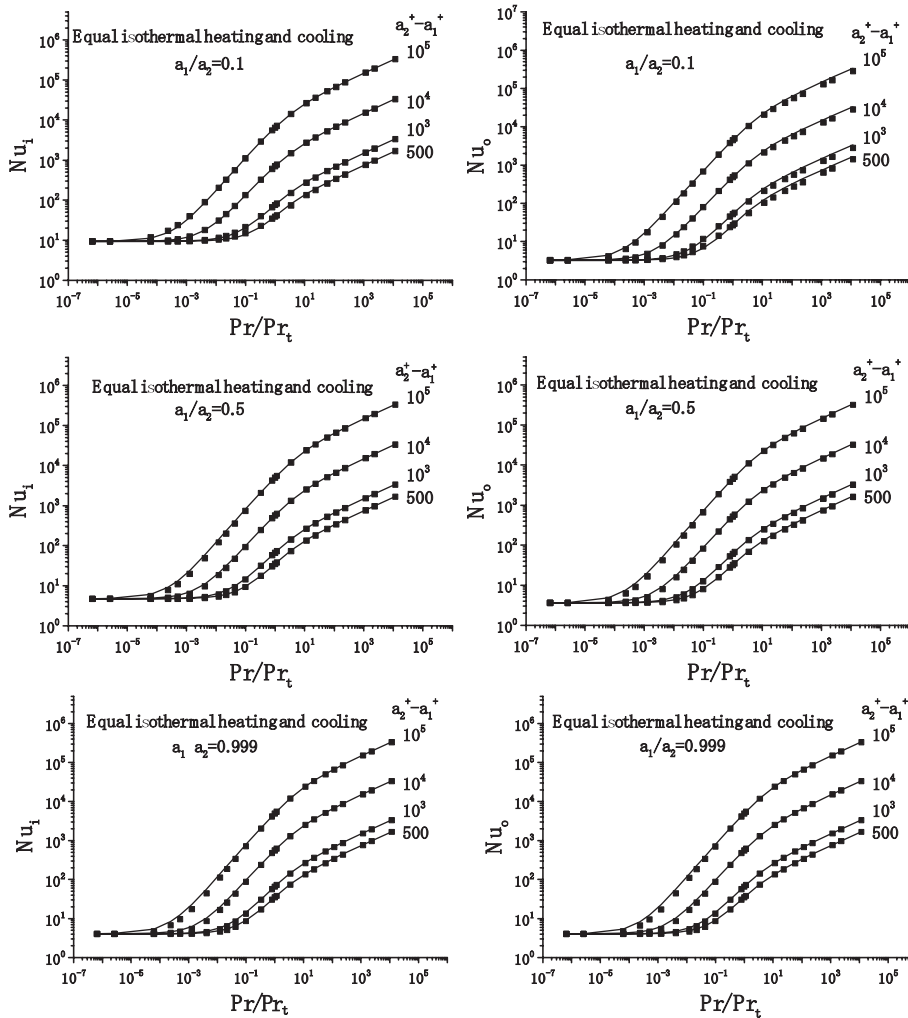


Fig. 3. Representation of the numerically computed values of Nu for equal uniform heating and cooling of the walls of an annulus by the predictive equations of Churchill and Zajic [3].

surroundings that effect as well. It may be observed in Table 12 that this ratio of temperature differences decreases with a decreasing aspect ratio and with a decreasing Prandtl number. It decreases very slowly with an increasing rate of flow for $Pr = Pr_t \cong 0.8673$, but, on the other hand, increases very slowly with increasing flow for $Pr = 0$.

6. Summary and conclusions

The results presented herein, when combined with those of Yu et al. [2] for heating of the inner wall, and generalized by superposition (Yu et al. [4]), encompass essentially all thermal boundary conditions that result in fully developed turbulent convection in annuli. The

computed values of Nu_0 and Nu_1 presented in tabular form herein are shown in Figs. 1–4 to be sufficient to predict with a high degree of accuracy the dependence of Nu on Pr/Pr_t for all values of $(a_2^+ - a_1^+)_{w1}$, all values of a_1/a_2 , and all thermal boundary conditions. Since Re bears a one-to-one correspondence to $(a_2^+ - a_1^+)_{w1}$ for a specified value of a_1/a_2 , these plots are an implicit test of the dependence on Re . At the same time, they confirm the accuracy and generality of the predictive equations of Churchill and Zajic [3]. A test of the validity and accuracy of the numerically computed values of Nu is provided in the comparisons with experimental data in Figs. 5 and 6. In view of the limited data for such thermal boundary conditions, the comparisons by Yu et al. [2] of the predictions of numerical computations using the same model with the much more extensive experimental

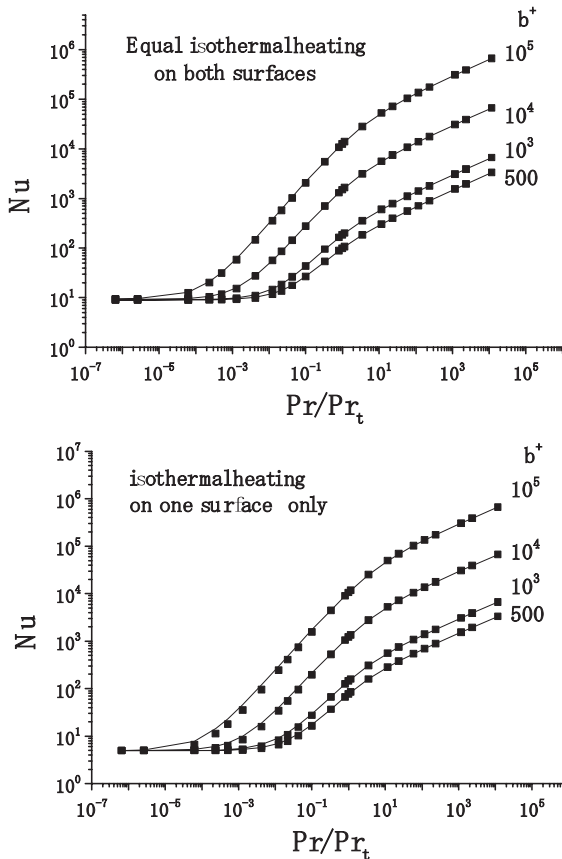


Fig. 4. Representation of the numerically computed values of Nu for equal uniform heating and cooling of the walls of an annulus by the predictive equations of Churchill and Zajic [3].

data for uniform inner heating, and the theoretical credentials of the modeling are perhaps more assuring.

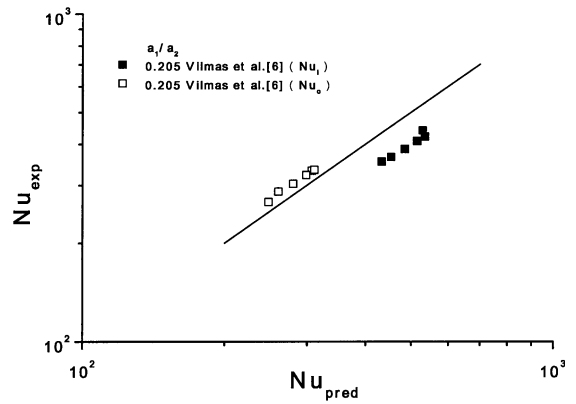


Fig. 6. Comparison of predicted and experimental values of Nu for annuli uniformly heated on both walls with $(j_{w1}a_1)/(j_{w2}a_2) = 1.29$.

Acknowledgment

The authors gratefully acknowledge the contribution of Dr. Masayuki Kanada in the preliminary formulation and the numerical computation of turbulent convection in annuli.

References

- [1] M. Kaneda, B. Yu, H. Ozoe, S.W. Churchill, The characteristics of turbulent flow and convection in concentric circular annuli. Part I. Flow, *Int. J. Heat Mass Transfer* 46 (26) (2003) 5045–5057.
- [2] B. Yu, Y. Kawaguchi, M. Kaneda, H. Ozoe, S.W. Churchill, The characteristics of turbulent flow and convection in concentric circular annuli. Part II. Uniform heating on the inner surface, *Int. J. Heat Mass Transfer*, doi:10.1016/j.ijheatmasstransfer.2004.08.022.

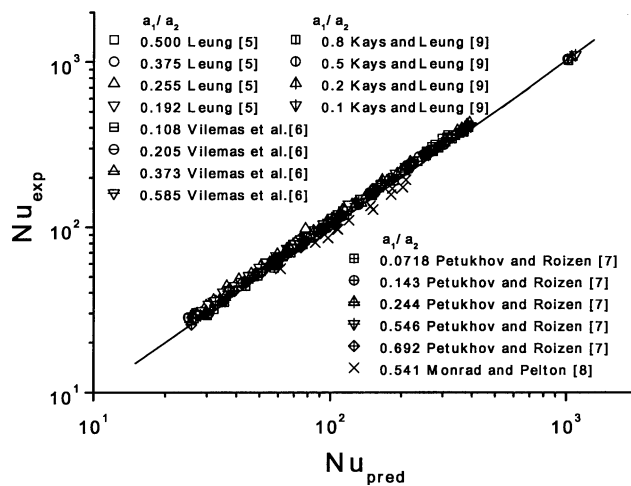


Fig. 5. Comparison of predicted and experimental values of Nu for annuli uniformly heated on the outer wall.

- [3] S.W. Churchill, S.C. Zajic, Prediction of fully developed convection with minimal explicit empiricism, *AIChE J.* 48 (5) (2002) 927–940.
- [4] B. Yu, Y. Kawaguchi, H. Ozoe, S.W. Churchill, The characteristics of turbulent flow and convection in concentric circular annuli. Part IV. Generalizations (in review).
- [5] E.Y.W. Leung, Heat transfer with turbulent flow in concentric and eccentric annuli with constant and variable heat flux, Ph.D. Thesis, Stanford University, Palo Alto, CA (1962), or see E.Y. Leung, W.M. Kays, W.C. Reynolds, Rept. AHT-4, Thermal Sciences Division, Dept. of Mechanical Engineering, Stanford University, Palo Alto, CA (1962).
- [6] J. Vilemas, B. Cesna, A. Zukauskas, J. Karni, *Heat Transfer in Gas-Cooled Annular Channels*, Hemisphere Publ. Corp., Washington, D.C., 1987.
- [7] B.S. Petukhov, L.I. Roizen, An experimental investigation of heat transfer in a turbulent flow of gas in tubes of annular section, *High Temperature* 1 (3) (1963) 373–380, Transl. from Russian by Consultants Bureau.
- [8] C.C. Monrad, J.F. Pelton, Heat transfer by convection in annular spaces, *Trans. Am. Inst. Chem. Engrs.* 38 (1942) 593–611.
- [9] W.M. Kays, E.Y. Leung, Heat transfer in annular passages—hydrodynamically developed turbulent flow with arbitrarily prescribed heat flux, *Int. J. Heat Mass Transfer* 6 (1963) 537–557.
- [10] S.W. Churchill, A reinterpretation of the turbulent Prandtl number, *Ind. Eng. Chem. Res.* 41 (25) (2002) 6393–6401.
- [11] B. Yu, H. Oxoe, S.W. Churchill, The characteristics of fully developed turbulent convection in a round tube, *Chem. Eng. Sci.* 56 (2001) 1781–1800.